Real-time and simultaneous measurement of tricuspid orifice and tricuspid anulus areas in anesthetized dogs

K Tamiya, M Higashidate and S Kikkawa

Circ. Res. 1989;64;427-436
Circulation Research is published by the American Heart Association. 7272 Greenville Avenue, Dallas, TX 72514
 Print ISSN: 0009-7330. Online ISSN: 1524-4571

Real-Time and Simultaneous Measurement of Tricuspid Orifice and Tricuspid Anulus Areas in Anesthetized Dogs

Kouichi Tamiya, Masafumi Higashidate, and Sho Kikkawa

Tricuspid valve orifice and tricuspid valve anulus areas were measured simultaneously in the anesthetized dog with a newly developed area-measuring system based on electromagnetic induction. This system permitted real-time monitoring of the area enclosed by the edges of valve leaflets and by the juncture of the valve leaflet and the cardiac wall in situ, without artificial constraint to the valve motion. Right atrial and right ventricular pressures were measured with two catheter-tipped micromanometers. During control state, tricuspid valve orifice area (TOA) increased up to its peak [1.38±0.26 cm^2 (mean±SD)] coincidently with either atrial systole or rapid ventricular filling. Atrial contraction evoked distinct presystolic tricuspid anulus narrowing with concomitant slow TOA reduction. This slow TOA reduction began 30.0±16.1 msec before systolic atrioventricular pressure crossover, and the following rapid TOA decrease was completed 38.7±12.2 msec after systolic atrioventricular pressure crossover. TOA began to increase 48.4±30.4 msec before diastolic atrioventricular pressure crossover at the end portion of the isovolumic relaxation phase, opposing residual transvalvular pressure gradient (3.33±1.79 mm Hg). The slow presystolic TOA decrease was considered to be a reflection of the presystolic anulus narrowing caused by atrial systole. An isolated atrial contraction induced by administering 1 mg acetylcholine chloride into the atrioventricular node artery or by vagus nerve stimulation could produce complete valve closure. Even in an isolated atrial contraction, the inflection point that marks the boundary between slow "atriogenic" closure presumably due to anulus narrowing and rapid closure presumably due to hemodynamic force was easily identified. (*Circulation Research* 1989;64:427–436)

Although several ingenious fluid mechanical models[1–3] of atrioventricular (A-V) valve motion have been proposed, quantitative data that deals directly with A-V valve motion in terms of the instantaneous valve orifice area has not been available. Concerning nonregurgitant A-V valve closure, multiple theories involving "atriogenic" and "ventriculogenic" mechanisms have been proposed. The major theories among them are 1) A-V pressure reversal due to deceleration of the transmitral flow ("breaking-jet theory," Henderson and Johnson[1]), 2) vortices formation under valve leaflets (Bellhouse[2]), and 3) chordal tension during diastole (Rushmer et al[4]). The mechanism responsible for A-V valve closure must be more complicated than we expected. It must imply, at least, reduction or reversal of the A-V pressure gradient due to atrial relaxation, A-V anulus contraction, intravalvular muscle fiber shortening,[5] etc., in addition to the three theories described above. Tsakiris et al[6–8] measured changes in the distance between two lead markers sutured at edges of both mitral leaflets on x-ray cineangiogram and demonstrated that mitral leaflets begin to move toward the closed position before the QRS complex. According to the widely advocated explanation that the closure process is initiated through an interplay of fluid-dynamic forces and ventricular wall motion during the deceleration of the forward flow through the valve ("breaking-jet" theory[1,9]), A-V valve closure should begin coincidently with the onset of transmitral flow deceleration, that is, A-V pressure reversal. Yellin et al[10] focused on the temporal relation between transmitral flow measured with an electromagnetic flowmeter and valve motion registered on an M-mode echocardiogram. They reported that the onset of mitral valve closure preceded the onset of transmitral flow deceleration. Their hypothesis[10] on the initiation of A-V valve motion is as follows: Dia-

From the Departments of Surgical Science and Pediatric Cardiovascular Surgery (M.H.), The Heart Institute of Japan, Tokyo Women's Medical College, Tokyo, Japan.

Address for reprints: Kouichi Tamiya, MD, Department of Surgical Science, The Heart Institute of Japan, Tokyo Women's Medical College, 8-1 Kawadacho, Shinjuku, Tokyo 162, Japan.

Received May 13, 1987; accepted August 8, 1988.

stolic chordal restraint and a Venturi effect bring the valve leaflets into the appropriate position for vortex formation by shear at the valve surface (shedding vortex), then the breaking of the jet becomes incorporated for growing the vortex, preparing the valve for complete closure. A ventricular pressure rise due to ventricular systole drives the valve toward closure, and the forward flow momentum will prevent regurgitation at final closure. Furthermore, they argued that it is impossible for the incoming jet to strike the ventricle apex and sweep up the ventricular walls to form the ring vortex, as described by Bellhouse,[2] in time to move the valve toward closure. Both studies[8,10] agreed on the point that the transmitral flow ceased (therefore, complete valve closure occurs) 20–40 msec after systolic A-V pressure crossover (SPCO). Tsakiris et al[8] reported an early onset of valve opening (5–60 msec) that opposed the A-V pressure gradient at the end-portion of the isovolumic relaxation phase, in disagreement with previous reports.[11–13] Thus, the mechanism and temporal relation of A-V valve opening is still controversial. Understanding the complexity of the mechanism governing A-V valve motion requires further physiological data on A-V valve movement using various measuring techniques.

Recently, we reported a new technique that permits real-time determination of the valve anulus area using electromagnetic induction and lock-in amplification.[14] Minor improvement of the technique enables simultaneous measurement of the A-V valve orifice area and the valve anulus area in situ. This technique provides not only precise determination of valve orifice/anulus areas but also restraint free valve movement, with a superb signal-to-noise ratio and a reasonable frequency response. This is the first experimental report in which the phasic variations in tricuspid valve orifice area (TOA) and tricuspid valve anulus area (TAA) with high-fidelity right atrial (RAP) and right ventricular (RVP) pressures were measured quantitatively and simultaneously in situ.

Materials and Methods

Seven mongrel dogs weighing 10.0–18.0 kg were anesthetized with intravenous pentobarbital sodium (30 mg/kg) and ventilated with a pressure-controlled artificial ventilator (model Mark-8, Bird Corp, Palm Springs, California). A midsternotomy was performed, and the heart was secured in a pericardial cradle. Figure 1 shows the conceptual framework of the present experiment. A right heart bypass was established as follows: 1) Whole venous blood return was collected into a funnel through two blood drainage cannulae introduced in advance into the superior and inferior venae cavae (SVC and IVC) via the azygous and femoral veins, respectively; 2) a short segment of synthetic Dacron vessel was sutured end-to-side to the main pulmonary artery, and then the venous blood was returned from the collecting funnel to a debubbling reservoir by a roller pump and returned to the pulmonary artery via the Dacron graft; 3) a bloodless right atrium was obtained by placing snares on the proximal pulmonary artery, SVC and IVC; 4) blood from the coronary sinus was removed by a suction pump. During the right heart bypass (lasting 15–20 minutes), the right atrial incision and the following surgical procedures were carried out. In some dogs, visible filariae in the heart were removed. One end of the metal thread, which had a nontraumatic needle on each end, was introduced into the right atrial cavity in the anteroseptal commissure marked by the fan chorda of the small papillary muscle of the conus. The edges of the anterior and posterior leaflets were stitched with the metal thread, then the thread was brought out of the right atrium in the commissure between the septal and posterior leaflets. Another end of the metal thread was introduced into right atrial cavity in the same entry (anteroseptal commissure), the margin of the septal leaflet was stitched, then the thread was brought out in the same exit (posteroseptal commissure). At the posteroseptal commissure side, both ends of the metal thread were tightly twisted together to avoid extra loop area formation and connected to a preamplifier made of a high-frequency operational amplifier (model NE592, Signetics Co, Sunnyvale, California) by soldering with a piece of fine shielded wire. The visible juncture of the valve leaflets and the cardiac wall was stitched with another metal thread to measure TAA simultaneously.

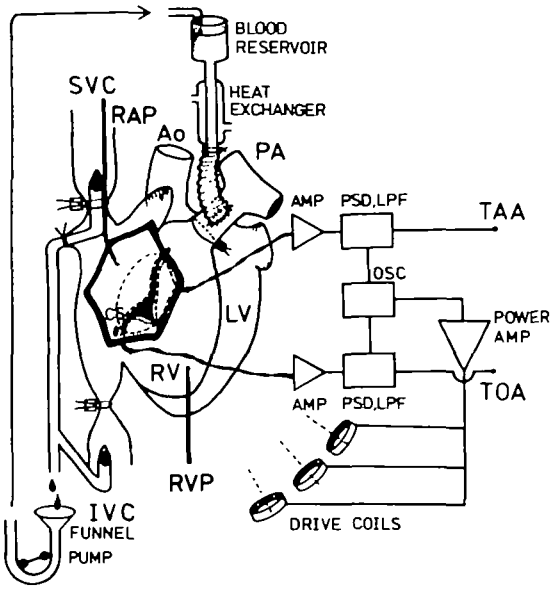

FIGURE 1. *Schematic diagram of experimental apparatus during right heart bypass. RAP, RVP, right atrial/ventricular pressure; SVC, IVC, superior/inferior vena cava; CS, coronary sinus; RV, LV, right/left ventricle; Ao, aorta; PA, pulmonary artery; AMP, amplifier; PSD, phase-sensitive detector; LPF, low pass filter; OSC, oscillator; TAA, tricuspid anulus area; TOA, tricuspid orifice area.*

Area-Measuring System

The area-measuring system developed for the present study is described in detail in a previous report.[14] Briefly, three carrier signals of constant magnitude were supplied for three drive coils assembled on a plywood base. The axes of the three coils, which were directed toward the tricuspid valve, intersected with each other at vertically opposite 20° angles. According to the procedure mentioned above, the tricuspid valve orifice and anulus were encircled with two pieces of extremely fine pliable metal thread made of four urethane-resin coated copper wires (25 μm diameter, Urernett wire, Sumitomo Denko, Osaka, Japan) during the right heart bypass. The infinitesimal three electrical potentials (roughly 5–10 μV), induced in the sense loop, were amplified with three lock-in amplifiers that consisted of phase-sensitive detectors (model AD630KN, Analog Devices, Inc, Norwood, Massachusetts) and low-pass filters (model UAF-41, Burr Brown Corp, Tucson, Arizona) having 50-Hz cutoff frequencies and −18 dB/oct gain slopes.

The total group delay time of the low-pass filter is approximately 5 msec for a 5–30 Hz sine-wave signal, which corresponds to the lag of 0.5 mm on the chart that runs at a speed of 100 mm/sec. The electrical potentials of each frequency induced in the sense loop consist of two components, one proportional to the rate of area change and the other proportional to the rate of field intensity change. The former is in phase when the carrier signal is chosen as the reference; the latter, which phase shifted 90°, is proportional to the sense loop area. In practice, the phase-sensitive detector produces 90° phase delay around the signal frequency of 100 kHz. The lock-in amplifiers effectively suppress the signals relating to the rate of area change when the phase-sensitive detectors are directly supplied with the carrier signals as a reference. Thus, the intensities of the three frequency signals detected by the present system are proportional to the projection area of the sense loop under conditions of a constant rate of change of the field intensity; this area is predominantly that of the tricuspid valve orifice.

Measurements were taken at end-expiratory points. Polarity was adjusted such that an upward deflection indicated increases in TOA or TAA. Replacement of the sense loop with the rigid metal triangle (made of three 2-cm brass rods, 1 mm in diameter), positioned at the tricuspid valve region, provides a standard signal (1.73 cm^2) for the calibration of the system. The TAA/TOA signals and other hemodynamic variables were recorded on the magnetic tape with a multichannel analog data recorder (model UFR-71460A, Sony Magnescale, Inc, Tokyo, Japan) at a tape speed of 38 cm/sec and reproduced later on a chart with a multichannel thermal array strip chart recorder (model WS682G, Nihon Kohden, Tokyo Japan; −3 dB at 1 kHz) at paper speeds of 100 or 200 mm/sec.

Other Measurements

Standard lead II electrocardiograms (ECG II) and aortic pressures (AoP) were recorded conventionally. Two catheter-tipped micromanometers (model PC-370, Millar, Houston, Texas) were introduced into the right atrium and right ventricle via the external jugular vein and apical puncture, respectively. Additional fluid-filled pressure manometry was carried out in the right atrium in order to calibrate the other catheter-tipped manometers against atmospheric pressure. The offset balance of the three manometers (one fluid-filled, two catheter-tipped) were adjusted to show the identical value at the end portion of the artificially induced prolonged asystole. To provide a sufficient duration of diastole for the rebalance of the two catheter-tipped manometers, rectangular electrical pulses of various amplitude (5 msec width, 30 Hz) were applied to the right cervical vagus nerve. The artificial asystole was repetitively induced to confirm the matching of two catheter-tipped manometers. To evaluate the effects of an increase in the right heart volume, a rapid blood transfusion (300 ml within 3 minutes) or pulmonary artery constriction was carried out. For a decrease in right heart volume, venous inflow occlusion was employed. To test the effects of enhanced myocardial contractility, bolus administration of isoproterenol (1 μg, 3 μg) was carried out. Ventricular pacing was employed to examine the effects of isolated ventricular contraction without preceding atrial systole on TAA/TOA. To evaluate the effects of isolated atrial contraction, reversible complete A-V block was created temporarily by the direct administration of acetylcholine chloride (1 mg) into the A-V node artery via the right coronary artery.

Results

From the top of Figure 2, ECG II, AoP, RAP measured with fluid-filled manometer, superimposed right ventricular and atrial pressures (RVP/RAP) measured with catheter-tipped micromanometers, and TAA/TOA areas are demonstrated. A slight increase in TOA with a concomitant increase in the transvalvular pressure gradient appears at the onset of right atrial systole. After the first peak (A) due to atrial systole, TOA decreases gradually at first, then rapidly. A distinct inflection point (B), which marks the boundary between slow and fast valve closures, appears at about one-half of total TOA excursion. The former slow "atriogenic" portion (A–B) should be attributed to the atrial activity since there was no ventricular action at that time. The latter fast "ventriculogenic" portion (B–C) may be attributed to rapid ventricular pressure rise due to ventricular contraction. A concomitant TAA decrease (A′ in this article and A in our previous report[14]) beginning about 60 msec before systolic A-V pressure crossover (SPCO) is remarkable in Figure 2, suggesting a significant role of anulus narrowing due to atrial contraction in the early onset of presystolic "atriogenic" valve closure.

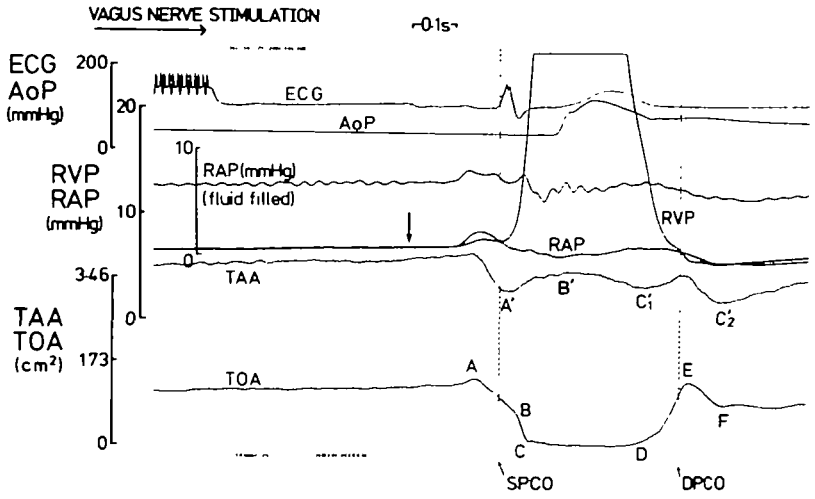

FIGURE 2. *High-speed recordings of (from the top) ECG II, aortic pressure (AoP), right atrial pressure (RAP) measured with conventional fluid-filled manometer, RAP and right ventricular pressure (RVP) measured with catheter-tipped micromanometers superimposed, tricuspid valve anulus area (TAA), and tricuspid valve orifice area (TOA) on same scale after prolonged diastasis. Leftmost spikes on ECG recording are artifact of vagus nerve stimulation. A', B', C_1', and C_2' on TAA recording are from a previous publication.[14] A, peak of TOA due to atrial systole; B, inflection point between slow "atriogenic" closure and rapid "ventriculogenic" closure; C, point of complete valve closure; D, beginning point of valve opening; E, peak due to rapid ventricular filling; F, valley of mid-diastolic closure; SPCO, systolic pressure crossover; DPCO, diastolic pressure crossover. The downward arrow indicates coincidence of two pressure recordings after prolonged diastasis. Note that RVP still overcomes RAP at the instant of valve opening.*

During the ventricular ejection phase (C–D), TOA remains zero while TAA shows a dome-shaped increase (B'). At the instant that the tricuspid valve begins to open at the end portion of the isovolumic relaxation phase (D), RVP still exceeds RAP by 6–8 mm Hg. As TOA tracing in this phase shows gradual change ("initial leaflet separation" after Tsakiris et al[8]), it is not easy to point out an accurate onset of valve opening. However, TOA is always larger than about 30% of its maximum value at the diastolic A-V pressure crossover (DPCO), and the onset of valve opening occurs about 90 msec before DPCO in Figure 2. To guarantee the time accuracy, measurements involving the pressure crossover points were carried out just after the artificially prolonged asystole, in which matching of two pressure gauges was checked. Thus, the temporal relation may be subject to the effects of vagus nerve stimulation (e.g., impaired atrial contractility,[15] impaired ventricular relaxation at the time of reperfusion,[16] etc.). This manometer calibration procedure is based on the assumption that no residual transvalvular flow existed at the end portion of a sufficiently prolonged diastole. During the rapid filling phase, TOA increases up to its second peak and (E) then begins to decrease while RAP still exceeds RVP (E–F). During mid-diastole, in which TOA decreases, the tricuspid valve motion shows

TABLE 1. **Control Values of Tricuspid Valve Anulus/Orifice Areas and Relevant Parameters in Seven Dogs**

Dog	Body wt (kg)	Heart rate (beats/min)	RVP (mm Hg)	Peak TAA (cm^2)	Peak TOA (cm^2)	Peak opening speed (cm^2/sec)*	Peak closing speed (cm^2/sec) (atriogenic/ventriculogenic)†
1	10	75	22	2.2	1.5	10.8	−14.1/−55.2
2	18	114	29	3.6	1.8	14.0	−9.7/−49.8
3	15	88	27	3.1	1.3	14.3	−12.9/−37.9
4	15	138	22	2.5	1.5	16.5	−8.7/−23.2
5	14	81	29	3.3	1.2	18.4	−6.9/−43.9
6	13	159	28	2.6	1.1	12.6	−13.4/−22.1
7	12	144	26	2.0	1.1	20.6	−8.1/−27.1
Mean	13.9	114.1	26.1	2.76	1.38	15.31	−10.98/−40.34
±SD	2.5	33.6	3.0	0.59	0.26	3.40	2.94/12.07

RVP, right ventricular pressure; TAA, tricuspid valve anulus area; TOA, tricuspid valve orifice area.
*Peak opening speed denotes slope of DE in Figure 2.
†Atriogenic/ventriculogenic closing speed denotes slopes of AB and BC, respectively, in Figure 2.

TABLE 2. Time Intervals Between Atrioventricular Pressure Crossover and the Onset of Tricuspid Valve Orifice Area Change

Dog	Time from SPCO to DPCO (msec)	Time from peak TOA (A) to SPCO (msec)	Time from SPCO to zero TOA (C) (msec)	Time from onset of TOA increase (D) to DPCO (msec)	Pressure difference at onset of TOA increase (D) (mm Hg)	Time from DPCO to peak TOA (E) (msec)
1	295	14	40	25	3.6	172
2	365	30	45	80	6.4	65
3	357	45	52	49	2.5	50
4	415	55	15	100	5.0	55
5	410	18	47	28	1.8	81
6	240	35	32	20	1.5	120
7	352	13	40	37	2.5	80
Mean	347.7	30.0	38.7	48.4	3.33	89.0
±SD	62.2	16.1	12.2	30.4	1.79	43.3

SPCO, systolic A-V pressure crossover; DPCO, diastolic A-V pressure crossover; TOA, tricuspid valve orifice area. Values that denote time intervals involving TOA change were corrected for the group delay time in the lock-in amplifiers (5 msec). These values are obtained from the cardiac cycle two to three beats after the cessation of vagus nerve stimulation to avoid error due to manometer offset drift.

complex oscillation, indicating that there is, superimposed on the basic mechanical events of valve closure, a resonating system with a fundamental frequency of about 10 Hz. Hemodynamic data and other variables relevant to TAA/TOA values are summarized in Table 1. The temporal relation between SPCO/DPCO points and the onsets of valve closure/opening are summarized in Table 2. Values involving the timing of TOA change have been corrected for the group delay time (less than 5 msec for 5–30 Hz sine wave) in the lock-in amplifier.

Effects of Volume Loading

To test the effects of volume loading on TOA, a rapid intravenous blood transfusion of 300 ml was carried out within 3 minutes via the IVC cannula (Figure 3). Volume expansion produced not only an increase in peak TOA during the rapid filling phase but also augmented peak TOA during atrial systole. So-called "E–F slope" steepened as cardiac output increased.[13] TAA was more sensitive to preload increase than TOA. As seen in Figure 3 diastolic TAA increase due to volume expansion was more dominant than that during systole since compliance of the myocardium surrounding the tricuspid valve anulus decreased during ventricular systole. As a result, TAA during diastole overcame that during systole after the 300-ml blood infusion. This phenomenon was also observed during pulmonary artery constriction (the rightmost column of Figure 4).

Effects of Venous Inflow Occlusion and Pulmonary Artery Constriction

The second column of Figure 4 shows effects of venous inflow occlusion on TAA and TOA. While two snares around SVC and IVC were ligated, TOA showed almost no change while TAA still demonstrated an incisure (A′) due to atrial contraction and

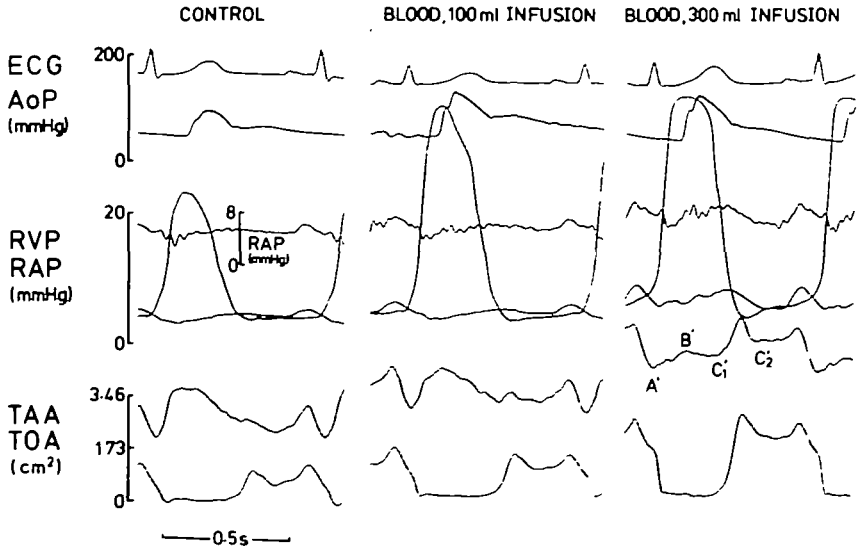

FIGURE 3. *Effects of rapid blood transfusion on phasic changes in tricuspid valve anulus area (TAA) and tricuspid valve orifice area (TOA). Distinct increase in mean TAA is remarkable after 300 ml blood infusion within 3 minutes. Diastolic TAA is more sensitive to volume expansion than that during systole. AoP, aortic pressure; RVP, right ventricular pressure; RAP, right atrial pressure; A′, B′, C_1′, and C_2′ are from a previous publication.*[14]

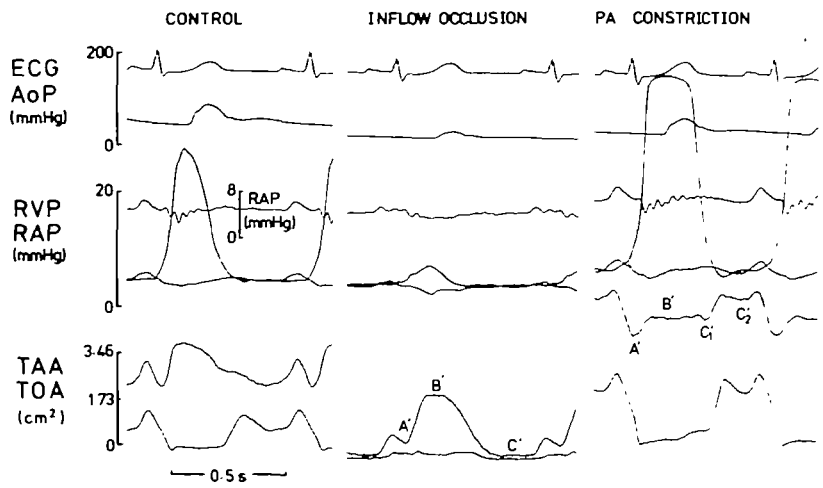

FIGURE 4. *Effects of venous inflow occlusion (middle) and pulmonary artery constriction (right) on tricuspid valve anulus area (TAA) and tricuspid valve orifice area (TOA). TAA vigorously fluctuates under conditions of no blood filling into right ventricle, while TOA shows almost no change during venous inflow occlusion. Note that TAA and TOA traces fall to zero during diastole under conditions of almost no blood filling into the heart. Increase in ejection resistance by pulmonary artery (PA) constriction prevents reduction in TAA at the end portion of systole. AoP, aortic pressure; RVP, right ventricular pressure; RAP, right atrial pressure; A', B', C', C_1', and C_2' are from a previous publication.*[14]

a hump (B') due to ventricular contraction. This suggests that TAA is governed by the myocardial activity around the valve anulus and TOA is not. During pulmonary artery constriction (the rightmost column in Figure 4), TAA elevated up to 5.5–6.0 cm^2 while TOA increased up to 2.6 cm^2. In cases of ventricular enlargement such as rapid blood transfusion (the rightmost column of Figure 3) or PA constriction (the rightmost column of Figure 4), maximum TAA values were attained during ventricular diastole, in contrast to the systolic maximum TAA value (B') during control. This phenomenon should be ascribed to reduced ventricular compliance during ventricular systole.

Effects of Artificial Pacing

Cardiac pacing was carried out to evaluate the effects of the lack of pertinent atrial systole on tricuspid valve motion. A complete valve closure was achieved by atrial pacing as shown in the TOA tracings of Figure 5 (second column). Atrial pacing produced TAA/TOA patterns similar to those during control except for the broadening of the "atriogenic" incisure of TAA compared with that of sinus rhythm. Ventricular pacing caused no "atriogenic" presystolic TAA narrowing, an incomplete reduction of TOA, and an abnormal RAP elevation, suggesting tricuspid regurgitation throughout the systole (the third column of Figure 5). The RAP elevation may be attributed to delayed atrial contraction due to retrograde A-V conduction. In contrast to normal sinus rhythm and atrial pacing, tricuspid valve closure starts about 40 msec after SPCO (third column, Figure 5) in ventricular pacing. Atrioventricular dual stimulation seems to improve prepositioning of tricuspid valve cusps since an increase in closing velocity of the tricuspid valve and a reduction in residual TOA during the ejection phase were observed. Preceding atrial activation by A-V sequential pacing, which is not

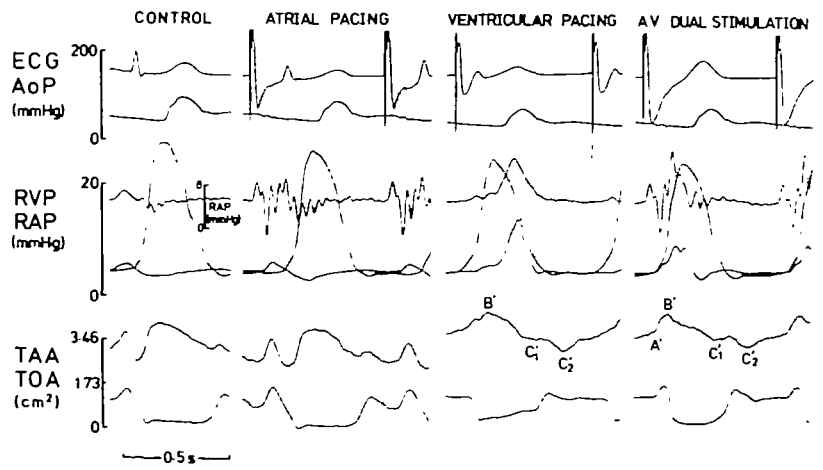

FIGURE 5. *Effects of various kinds of artificial pacing on tricuspid valve anulus area (TAA) and tricuspid valve orifice area (TOA). Atrial pacing (second column) produced normal contraction/relaxation pattern of TAA/TOA except a broadening of A' valley in TAA tracing. Conventional right ventricular pacing (third column) produced distinct valve reopening during ejection phase with concomitant RAP elevation suggesting tricuspid regurgitation. Simultaneous atrial stimulation with ventricular stimulation (rightmost column) seemed to improve valve coaptation. A notch corresponding to A' appears in TAA tracing. Atrioventricular sequential pacing is not included here. AoP, aortic pressure; RVP, right ventricular pressure; RAP, right atrial pressure; A', B', C_1', C_2' are from a previous publication.*[14]

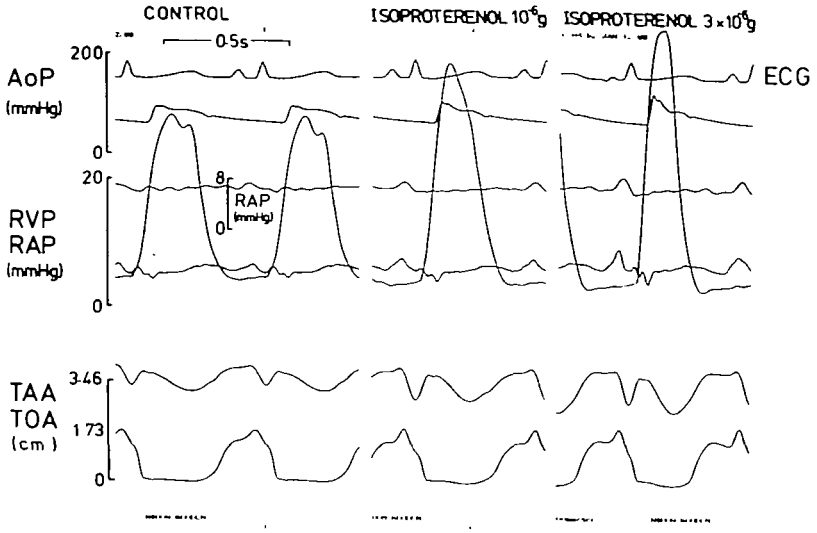

FIGURE 6. *Effects of isoproterenol infusion on tricuspid valve anulus area (TAA) and tricuspid valve orifice area (TOA). Isoproterenol infusion accelerates heart rate and enhances both atrial and ventricular myocardial contractility. Increase in magnitudes of presystolic TAA narrowing and systolic reduction in TAA are evident. In spite of TAA reduction, peak TOA remains practically constant. AoP, aortic pressure; RVP, right ventricular pressure; RAP, right atrial pressure.*

included in the figure, effectively minimized the elevation of TOA during the ejection phase and improved systolic regurgitation.

Effects of Isoproterenol Infusion

The administration of isoproterenol (1 or 3 μg i.v.) effectively enhanced heart rate and myocardial contractility. As a result of increased heart rate, the first peak of TOA at atrial systole and the second peak of TOA during the rapid filling phase merged into one. The enhanced atrial contractility augmented the "atriogenic" presystolic TAA narrowing and reduced mean TAA value that reflected the decreased ventricular volume (Figure 6).

Effects of Electrical Vagus Nerve Stimulation

In our preliminary study using lead markers and cinefluorography, it has been proved that a combination of sinus node disabling and electrical ventricular pacing leads to abnormal movement of the septal leaflet. Therefore, we employed electrical right vagus nerve stimulation to examine the effects of bradycardia and prolonged asystole although vagus nerve stimulation impairs atrial contractility.[15] At the end portion of sufficiently prolonged diastasis by vagus nerve stimulation with semi-open valve position (e.g., as indicated by a downward arrow in Figure 2), RAP and RVP are expected to equalize. Thus, we confirmed appropriate offset adjustments of the two catheter-tipped micromanometers in the right atrium and ventricle. A complete tricuspid valve closure after an isolated atrial systole was observed during right cervical nerve stimulation in an experimental series using venous inflow occlusion for the installation of the metal thread (not included in Tables 1 and 2, but see Figure 7). Zero TOA value and about 250 msec sustained A-V pressure reversal (Figure 7, downward arrow) indicate complete tricuspid valve closure. Venous blood return to the right atrium gradually raises RAP, and increasing ventricular volume moves the equilibrium position of tricuspid valve leaflets toward the open position.

Effects of Isolated Atrial Contraction

In the present experiment, acetylcholine chloride administration (1 mg) into the A-V node artery was employed to examine the effects of isolated atrial contraction on the tricuspid valve motion. After the onset of RAP increase in the isolated atrial contrac-

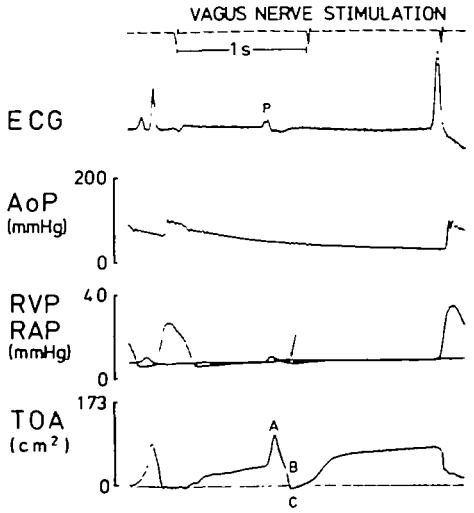

FIGURE 7. *Effects of isolated atrial contraction during vagus nerve stimulation on tricuspid valve orifice area (TOA). This trace shows an evidence of complete tricuspid valve closure after isolated atrial systole unaccompanied by ventricular activity. This was obtained in an experimental series, not included in the tables, using venous inflow occlusion for installation of metal thread. The downward arrow denotes sustained A-V pressure reversal. P, P wave; AoP, aortic pressure; RVP, right ventricular pressure; RAP, right atrial pressure; A, peak of TOA due to atrial systole; B, inflection point between slow "atriogenic" closure and rapid "ventriculogenic" closure; C, point of complete valve closure.*

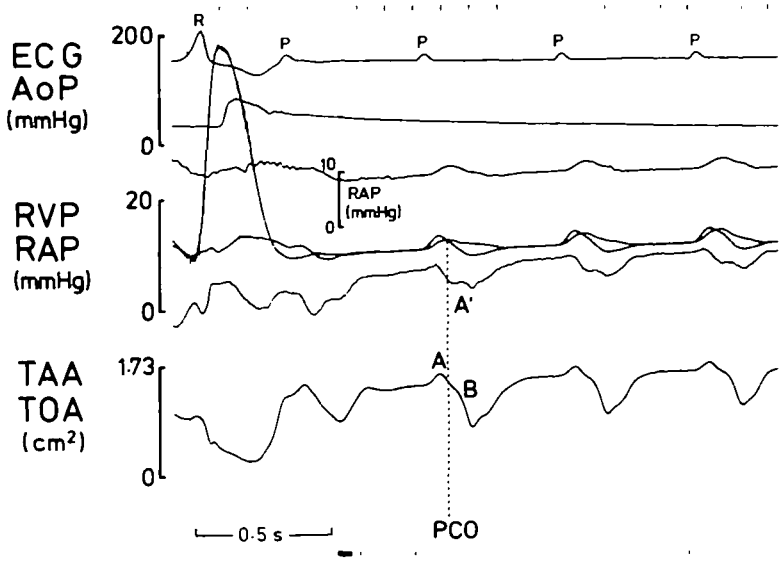

FIGURE 8. *Effects of isolated atrial contraction on tricuspid valve anulus area (TAA) and tricuspid valve orifice area (TOA). A-V block was created by the administration of 1 mg acetylcholine chloride into A-V node artery. R, R wave; P, P wave; PCO, atrial diastolic pressure crossover. AoP, aortic pressure; RVP, right ventricular pressure; RAP, right atrial pressure; A', from a previous publication[14]; A, peak of TOA due to atrial systole; B, inflection point between slow "atriogenic" closure and rapid "ventriculogenic" closure.*

tion (Figure 8), TOA increases up to its peak (A), then begins to fall, but fails to reduce down to zero. During the time between peak RAP and pressure crossover (PCO), TOA decreases even though RAP exceeds RVP. This suggests that TOA decreases in opposition to the A-V pressure gradient, presumably owing to valve anulus narrowing during the early stage of tricuspid valve closure. An inflection point (B) that marks the boundary between slow and rapid TOA decrease is observed, and TOA begins to decrease rapidly even after TAA ceases decreasing. Therefore, the latter rapid TOA reduction should be attributed to a hemogenic mechanism, that is, A-V pressure reversal due to atrial relaxation.

Discussion

As autopsy showed the metal threads to be properly placed as described above, it could be concluded that the recorded area signals accurately reflected the TAA/TOA and that the movements of the tricuspid valve and tricuspid anulus were not altered by the procedure. However, the metal threads, particularly those placed on the edges of the anterior and posterior leaflets, tend to be anchored to chordal insertions since they are more durable than the free edges of the leaflets. In addition, coaptation of the leaflets occurs such that they make a contact zone. Therefore, the traction of the chordae tendineae, which is assumed to be an important factor for the explanation of early mitral opening in the "myogenic" theory of mitral opening,[17–19] would move the wire loop outward while the valvular edges are still approximated. Thus, neither zero TOA nor nonzero TOA may afford an accurate prediction of the leaflet edge approximation. Furthermore, wire loop plane rotation (though we paid much attention to minimize the error due to it[14]) and overlap of the closed valve edge can result in alterations in the area signal. Actually, the area signal recorded in this method reflects "global" tricuspid orifice area. Therefore, the accuracy of the present technique is circumscribed, and further investigation on the exact timing of the A-V valve movement should be coupled with topical blood velocimetry at the leaflet edge.

Figure 9 schematically shows tricuspid valve motion with real traces of TAA, TOA, RVP, and RAP. In this figure, a 2.4 cm^2 downward shifted TAA trace was superimposed on the TOA trace (dashed line) to demonstrate a striking similarity between TAA and TOA traces during the presystolic "atriogenic" anulus narrowing (A–B). This suggests that "atriogenic" presystolic TAA narrowing due to appropriately timed atrial systole is a powerful candidate for the explanation of the early onset of A-V valve closure. The similarity between TAA and TOA also appeares during the "middiastolic closure," suggesting "myogenic" contribution to this phenomenon. Thus, the present study lends support to the active "myogenic" process for the explanation of the early onset of A-V valve closure and opening in addition to the conventional "hemogenic" mechanism.

The A-V valve in the intact animal, contrary to an artificial prosthetic mechanical valve of any kind, offers both very little impedance to the ventricular filling and valve closure[9] with negligible regurgitation. It has been inferred from the sustained reversal of A-V pressure difference after an isolated atrial activity in man[20,21] and experimental animals[15,22–24] with complete A-V block that the atrial contraction unaccompanied by ventricular systole leads to complete A-V valve closure. On the other hand, direct registration of the mitral leaflet motion by Tsakiris et al[6] showed that isolated atrial contraction led to slow and partial mitral valve closure of very short duration. The present study failed to demonstrate that an isolated atrial contraction always brought about complete tricuspid valve closure. However, complete tricuspid valve closure was observed after an isolated atrial activity during vagus nerve stimulation in

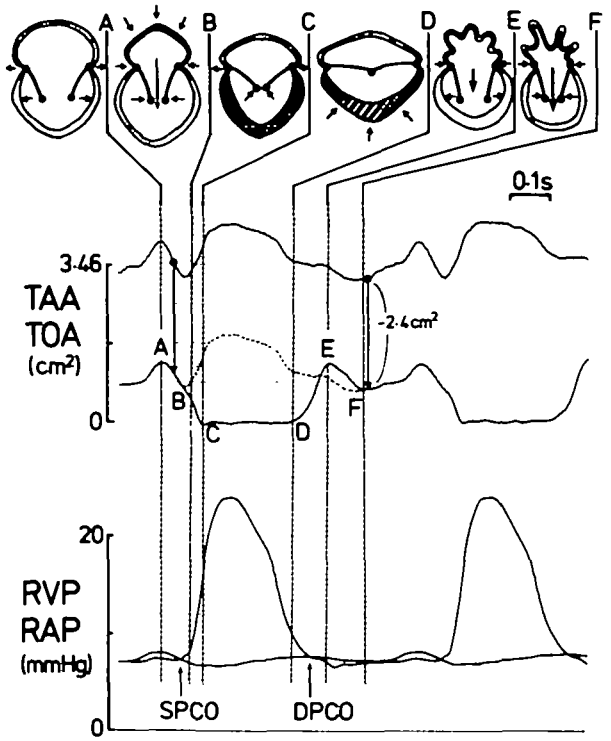

FIGURE 9. *Schematic drawings that summarize changes of tricuspid valve anulus area (TAA) and tricuspid valve orifice area (TOA) (upper panel) with TAA/TOA (middle panel) and RVP/RAP (lower panel) tracings. In middle panel, TAA shifted 2.4 cm² downward (dashed line) to illustrate similarity between TAA and TOA tracings during "atriogenic" presystolic TAA narrowing. RVP, right ventricular pressure; RAP, right atrial pressure; SPCO, systolic A-V pressure crossover; DPCO, diastolic A-V pressure crossover. A–B, presystolic anulus narrowing; B–C, ventricular contraction; C–D, ventricular ejection; D–E, ventricular relaxation; E–F, rapid ventricular filling; F–A, diastasis.*

the experiment using venous inflow occlusion for the installation of the metal thread (not included in tables, but see Figure 7). Increased ventricular volume, depressed atrial contractility, and abundant venous return seemed to retard complete valve closure after an isolated atrial contraction.

Since Dean[25] achieved direct registration of the mitral cusp motion, the preceding atrial activity has long been assumed to be a prerequisite for the regurgitation free valve closure.[26] On the other hand, several investigators[6,27–29] have said that properly timed atrial contraction is not necessarily essential for nonregurgitant mitral valve closure. In the present study on the direct measurement of TAA/TOA in open-chest, anesthetized dogs, ventricular pacing led to an incomplete reduction in TOA, disappearence of A′ notch from TAA trace, and abnormal RAP elevation, suggesting tricuspid regurgitation. Atrial pacing showed normal TOA pattern; therefore, the presystolic valve anulus narrowing showed its importance. It is, however, unclear whether nonregurgitant valve closure is accomplished through presystolic "atriogenic" TAA narrowing or "atriogenic" transvalvular flow (atrial kick), or both. To define the role of atrial systole in nonregurgitant A-V valve closure, further investigation involving the fixation of the tricuspid anulus with a rigid ring will be indispensable.

In diastole, two peaks of TOA, one due to rapid filling and the other due to atrial systole, were observed at a heart rate under approximately 90 beats/min. Peak values of TOA during atrial systole tended to overcome those during rapid filling in our experiment. An increased diastolic ventricular volume enhanced peak TOA at rapid filling. In the studies of intact dogs by Tsakiris et al,[6–8] peak mitral orifice diameter during rapid filling constantly exceeded that during atrial systole. The difference between the studies may be related to our different conditions: 1) abnormal right atrial transmural pressure due to the absence of pericardial constraint and open chest, 2) reduced cardiac output and higher heart rate (i.e., decreased ventricular volume) due to open chest and pentobarbital anesthesia, and 3) difference of anatomical shape between the tricuspid valve and the mitral valve. In other words, the diastolic suction of lesser compliant left ventricle phase may play a significant role in the rapid ventricular filling.

In conclusion, the importance of the presystolic closure of the A-V valve for nonregurgitant valve closure is not fully elucidated in the present study. However, direct simultaneous measurement of TAA and TOA clearly demonstrates several findings: 1) The shape of TAA during presystolic narrowing resembles that of TOA, suggesting an important role in nonregurgitant A-V valve closure; 2) TOA begins to decrease before the systolic A-V pressure crossover; 3) TOA begins to increase before the diastolic A-V pressure crossover; and 4) TOA reduced down to nearly zero solely as a result of an isolated atrial activity.

Acknowledgments

We are grateful to the members of the animal laboratory of The Heart Institute of Japan for their expert help and hearty encouragement and to Mr. Keizo Tanaka for his expertise on the medical instrumentation.

References

1. Henderson Y, Johnson FE: Two modes of closure of the heart valves. *Heart* 1912;4:69–82
2. Bellhouse BJ: Fluid mechanics of a model mitral valve and left ventricle. *Cardiovasc Res* 1972;6:199–210
3. Lee CSF, Talbot L: A fluid-mechanical study of the closure of heart valves. *J Fluid Mechanics* 1979;91:41–63
4. Rushmer RF, Finlayson BL, Nash AA: Movements of the mitral valve. *Circ Res* 1956;4:337–342
5. Sonnenblick EH, Napolitano LM, Daggett WM, Cooper T: An intrinsic neuromuscular basis for mitral valve motion in the dog. *Circ Res* 1967;21:9–15

6. Tsakiris AG, Gordon DA, Mathieu Y, Lipton I: Motion of both mitral valve leaflets: A cineroentgenographic study in intact dogs. *J Appl Physiol* 1975;39:359–366
7. Tsakiris AG, Gordon DA, Mathieu Y, Padiyar R, Labrosse C: Sudden interruption of leaflet opening by ventricular contractions: A mechanism of mitral regurgitation. *J Appl Physiol* 1976;40:132–137
8. Tsakiris AG, Gordon DA, Padiyar R, Fréchette D: Relation of mitral valve opening and closure to left atrial and ventricular pressures in the intact dog. *Am J Physiol* 1978;234: H146–H151
9. Parmley WW, Talbot L: Heart as a pump, in Berne RM, Sperelakis N, Geiger SR (eds): *Handbook of Physiology*, sec 2, vol 1. Bethesda, Md, American Physiological Society, 1979, pp 449–460
10. Yellin EL, Peskin C, Yoran C, Koenigsberg M, Matsumoto M, Laniado S, McQueen D, Shore D, Frater RWM: Mechanisms of mitral valve motion during diastole. *Am J Physiol* 1981;241:H389–H400
11. Laniado S, Yellin EL, Miller H, Frater RWM: Temporal relation of the first heart sound to closure of the mitral valve. *Circulation* 1973;47:1006–1014
12. Pohost GM, Dinsmore RE, Rubenstein JJ, O'Keefe DD, Grantham RN, Scully HE, Beierholm EA, Frederiksen JW, Weisfeldt ML, Daggett WM: The echocardiogram of the anterior leaflet of the mitral valve: Correlation with hemodynamic and cineroentgenographic studies in dogs. *Circulation* 1975;51:88–97
13. Laniado S, Yellin E, Kotler M, Levy L, Stadler J, Terdiman R: A study of the dynamic relations between the mitral valve echogram and phasic mitral flow. *Circulation* 1975;51:104–113
14. Tamiya K, Higashidate M, Kikkawa S: Technique with lock-in amplifier for real-time measurement of tricuspid valve annulus area. *Am J Physiol* 1986;251:H236–H241
15. Sarnoff SJ, Gilmore JP, Mitchell JH: Influence of atrial contraction and relaxation on closure of mitral valve. *Circ Res* 1962;11:26–35
16. Tyberg JV, Yeatman LA, Parmley WW, Urschel GW, Sonnenblick EH: Effects of hypoxia on mechanics of cardiac contraction. *Am J Physiol* 1970;218:1780–1788
17. Sovak M, Lynch PR, Stewart GH: Movement of the mitral valve and its correlation with the first heart sound: Selective valvular visualization and high-speed cineradiography in intact dogs. *Invest Radiol* 1973;8:150–155
18. Marzilli M, Sabbah HN, Lee T, Stein PD: Role of the papillary muscle in opening and closure of the mitral valve. *Am J Physiol* 1980;238:H348–H354
19. Steffens TG, Hagan AD: Role of chordae tendineae in mitral valve opening: Two-dimensional echocardiographic evidence. *Am J Cardiol* 1984;53:153–156
20. Zaky A, Steinmetz E, Feigenbaum H: Role of atrium in closure of mitral valve in man. *Am J Physiol* 1969; 217:1652–1659
21. Grant C, Greene DG, Bunnell IL: The valve-closing function of the right atrium. *Am J Med* 1963;34:325–328
22. Williams JCP, O'Donovan TPB, Vandenberg RA, Strum RE, Wood EH: Atriogenic mitral valve reflex: Diastolic mitral incompetence following isolated atrial systoles. *Circ Res* 1968;22:19–27
23. Little RC: Effect of atrial systole on ventricular pressure and closure of the A-V valves. *Am J Physiol* 1951;166:289–295
24. Brockman SK: Mechanism of the movements of the atrioventricular valves. *Am J Cardiol* 1966;17:682–690
25. Dean AL Jr: The movements of the mitral cusps in relation to the cardiac cycle. *Am J Physiol* 1916;40:206–217
26. Little RC: The mechanism of closure of the mitral valve: A continuing controversy. *Circulation* 1979;59:615–618
27. Braunwald E, Rockoff SD, Oldham HN Jr, Ross J Jr: Effective closure of the mitral valve without atrial systole. *Circulation* 1966;33:404–409
28. Williams JCP, Vandenberg RA, O'Donovan TPB, Strum RE, Wood EH: Roentgen video densitometer study of mitral valve closure during atrial fibrillation. *J Appl Physiol* 1968; 24:217–224
29. Vandenberg RA, Williams JCP, Strum RE, Wood EH: Effect of ventricular extrasystoles on closure of mitral valve. *Circulation* 1969;39:197–204

KEY WORDS • atrioventricular valve motion • tricuspid anulus/orifice area • breaking-jet theory • vortex formation • nonregurgitant valve closure